ISBN 978-81-936279-4-5
9th International Conference on Disaster Management, Building Design,Materials & Civil Engineering (DBMCE-18)
Antalya (Turkey) May 3-4, 2018

Identification of Reinforcement Corrosion in Large-Scale RC Beams with Acoustic Emission Sensing

Ahmed A. Abouhussien[1] and Assem A. A. Hassan[1]

[1]Department of Civil Engineering, Faculty of Engineering and Applied Science, Memorial University of Newfoundland, St. John's, Newfoundland and Labrador, Canada, A1B 3X5(Email: aabouhussien@mun.ca)

Abstract**:** *In this paper, the acoustic emission (AE) analysis was employed to identify early corrosion of reinforcing steel in reinforced concrete (RC) large-scale beams. These beams were exposed to localized accelerated corrosion procedures at one of the end sides of each beam. Five RC beams were corroded through an electrically accelerated corrosion process to reach 5, 10, 20, and 30% of steel mass loss. The beams were constantly monitored during the accelerated corrosion tests via half-cell potential (HCP) measurements and three attached AE sensors distributed along the span of the beam. During the test, the corrosion and cover crack initiation were monitored and the crack width measurements were daily attained. The results showed that the analysis of AE signal parameters acquired throughout the corrosion period enabled the detection of both corrosion and cover crack onset earlier than HCP readings and prior to any signs of visual cracking, regardless of sensor location. AE parameters examined in this paper (number of hits and cumulative signal strength (CSS) showed to be highly correlated with the level of corrosion damage.*

Keywords: *reinforcing steel corrosion, acoustic emission, beams, cracks*

1. Introduction

Corrosion of reinforcement steel is considered one of the major problems affecting the integrity of different concrete structures exposed to chlorides [1-5]. Corrosion causes severe deterioration in reinforced concrete (RC) structures, thus reducing the strength and expected service lifetime of exposed structures [6-10]. Early corrosion identification is required to achieve efficient planning and prioritizing of repair operations [11]. Consequently, efforts have been made by various researchers to develop innovative methodologies capable of early corrosion detection in RC structures. Meanwhile, there is an immediate need for the development of quantitative non-destructive testing (NDT) methods for the aim of determining the extent of corrosion to predict remaining capacity of existing RC structures.

The available standard NDT techniques used for corrosion monitoring include half-cell potential (HCP) and linear polarization resistance (LPR) methods [12-13]. The HCP technique enables the identification of the probability of corrosion activity of exposed reinforcing steel bars in RC structures. However, this method requires direct connection to the embedded bars and cannot determine the severity of corrosion activity. On the other hand, the LPR method is utilized to monitor the rate of corrosion in RC structures. Nonetheless, this method is based on assuming uniform corrosion of the reinforcing steel, which may contradict with the actual corrosion process in existing structures [13]. It should also be mentioned that, the previously mentioned NDT methods are both not suitable for real-time monitoring and are typically intrusive [14].

Acoustic emission (AE) technique is one of the available NDT methods that allow the detection of both the inception and progression of reinforcing steel corrosion [15-17]. A number of experimental investigations also used the AE monitoring methodology for evaluating other damage mechanisms in concrete. For instance, AE monitoring has been employed to evaluate the concrete-to-steel bond behaviour under pull-out tests [18-21] and

detect bond failure in the anchorage zone of RC beams [22-23]. However, the literature lacks information regarding corrosion monitoring of large-size RC beams using AE monitoring. The purpose of this paper is to verify the feasibility of AE monitoring in early corrosion and cover crack detection of large-scale RC beams using attached AE sensors based on AE analysis.

2. Experimental Program

2.1. Materials

Five large-scale RC beams were constructed and tested. All beams were constructed using one normal concrete mixture and ordinary deformed reinforcing steel bars. This concrete mixture contained type General Use Canadian Portland cement, similar to ASTM Type I, with a specific gravity of 3.15 [24]. Natural sand and 10 mm maximum size stone were incorporated into the mixture as fine and coarse aggregates, respectively. Both coarse and fine aggregates had a specific gravity of 2.60 and water absorption of 1%. The 28-day compressive strength of concrete was obtained by testing six cylindrical samples as per ASTM C39 [25]. Moreover, the splitting tensile strength of six additional cylindrical specimens was determined based on ASTM C496 [26], as seen in Table 1. Carbon steel bars with two variable diameters (10 and 20 mm) were used in all beams identified as 10M and 20M, respectively. All reinforcing steel bars have an average yield stress of 480 mega pascal (MPa) and tensile strength of 725 MPa. The mixture properties and 28-day compressive/tensile strength results of the concrete mixture are demonstrated in Table 1.

TABLE I: Mixture Proportions 28-Day Strength of Concrete

Cement (kg/m^3)	10 mm stone (kg/m^3)	Sand (kg/m^3)	Water (kg/m^3)	28-day compressive strength (MPa)	28-day splitting tensile strength (MPa)
350	1168.27	778.84	140	f_c = 40.38	f_{ct} = 3.79

2.2. Design of Beams

Five RC large-scale beams were constructed with two configurations: 250 x 250 x 1500 mm and 250 x 250 x 2440 mm were exposed to accelerated corrosion procedures to reach variable corrosion levels (5, 10, 20, and 30% of steel mass loss). These beams were also used in bond testing in another previous study, therefore were designed to ensure bond failure. All beam specimens were reinforced with two 20M steel bars as main reinforcement and 10M stirrups with the arrangement shown in Fig. 1. Two additional 10M bars were provided to hold the stirrups in each beam. The 20M main steel bars were partially debonded by the inclusion of polyvinyl chloride (PVC) pipes with a diameter of 1 in (bond breakers) along the bar except at the bonded parts of each bar (200 mm at the two ends of all beams). The space between the PVC pipes and the 20M main steel bars was sealed with a waterproof silicon filling before and after the bonded parts to completely isolate the un-bonded parts of the bar and to prevent them from corrosion.

To allow the connection to the power supply in the accelerated corrosion period, both the 20M bars contained two protruding parts (Fig. 1). Beams B1, B2, B3, and B4 had the same dimensions (250 x 250 x 1500 mm) and were corroded to 5, 10, 20, and 30% of steel mass loss, respectively. On the other hand, B5 was designed with identical cross section (250 x 250 mm), except with a longer length (2440 mm) and was exposed to 30% of steel mass loss. In all beams, concrete was cast in wooden formwork while the 20M reinforcing bars were horizontally placed at the bottom of the formwork. All beams were compacted through mechanical vibration. After 24 hours of casting, the beam specimens were de-molded and then water-cured for a period of 28 days before being exposed to the accelerated corrosion test.

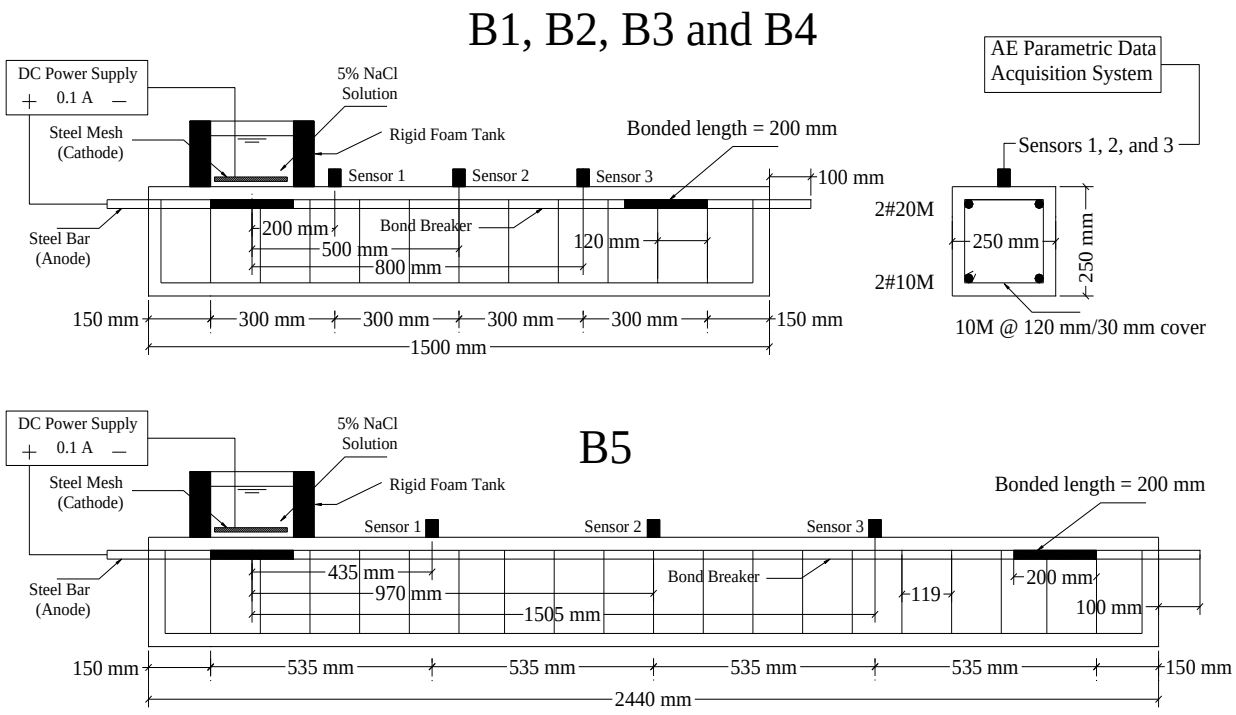

Fig. 1: Details of beams and test setup.

2.3. AE and Corrosion Test Setup

An electrically accelerated corrosion test was implemented so as to induce severe corrosion levels in a reasonable time frame. The test was performed using a constant electrical current (0.1 A) and varied corrosion periods to reach variable degrees of steel mass loss. The beams were subjected to corrosion at only one side along the bonded length (200 mm) of the two 20M main steel bars (Fig. 1) to represent localized corrosion condition. As being upside down, one end of each beam was exposed to a 5% sodium chloride (NaCl) water solution by means of a hard foam tank attached to the top of the beam surface along the bonded length. Both the 20M steel bars in each beam were connected to two direct current (DC) power supplies acting as anodes (+). In addition, a stainless steel mesh was positioned at the bottom of the foam tank to serve as cathodes (–).

Throughout the corrosion tests, the half-cell potential (HCP) test was daily executed and visual inspection of corrosion cracking was daily monitored. The HCP test was performed in accordance with the ASTM standard test method [27]. As soon as the corrosion cracks were identified, the crack width measurements were also daily obtained by means of a crack measuring microscope. The final corrosion crack widths were recorded at the end of the corrosion tests for the aim of correlation with the AE data. Besides, the actual percentages of steel mass loss were verified following the bond testing after breaking all beams and weighing the corroded parts of the steel bars according to ASTM G1 [28]. The weight of the corroded parts of the bars (200 mm length) was then compared with a reference un-corroded part having the same bar diameter and length to estimate the actual percentages of steel mass loss.

Each beam was monitored through the accelerated corrosion test via three AE sensors (Fig. 1). All sensors used in this investigation were piezoelectric AE sensors (R6I-AST) with integral preamplifier. These sensors were attached to the top side of the beam surface at the centre line of the beam cross section by a two-part epoxy adhesive (Fig. 1). These sensors were distributed at three varied distances from the corroded side of the beam. Four-channel AE data acquisition system and AEwin signal processing software were employed to acquire and collect the resulting acoustic emissions during all accelerated corrosion tests. An amplitude threshold level was setup at 40 (dB) to record the emitted AE signals through the corrosion exposure period. A number of AE signal parameters included amplitude, duration, and signal strength were continuously collected by the AE data acquisition system.

3. Results and Discussion

As mentioned before, the beams were subjected to four variable periods of accelerated corrosion process to reach four levels of corrosion in terms of steel mass loss (5%, 10%, 20%, and 30%). These levels of steel mass loss also yielded corrosion cover cracking at the exposed end of all beams, as can be seen from Table 2. All beams exhibited two cracks observed along the bonded length (subjected to chloride solution) of the two main bars (one crack at each beam side). Table 2 presents the maximum measured values of crack widths at the end of corrosion periods of all beams, which showed larger crack widths with higher percentage of steel mass loss. It can also be seen from Table 2 that the percentages of both the theoretical and actual steel mass loss indicated good agreement in all beams.

TABLE II: Results of Corrosion Tests

Beam	Theoretical mass loss (%)	Actual mass loss (%)	Exposure time (days)	Time to first crack (days)	Maximum crack width (mm)
B1	5	4.5	25	14	0.6
B2	10	9.2	34	15	0.9
B3	20	18.3	52	15	1.2
B4	30	27.9	70	15	2.5
B5	30	29.7	70	14	3.0

3.1. Early Corrosion Detection by AE Analysis

The variations in the number of hits and CSS were analyzed throughout the tests to detect corrosion initiation in all beams. Figs. 2 and 3 represent the typical variations of these AE parameters for Sensor 2 of B1, as an example for all other beams. It can be seen from these figures that the values of number of hits and CSS witnessed an overall increase until the end of corrosion period. This overall increase in these AE parameters can be attributed to both corrosion initiation and propagation in the exposed parts of the steel bars reaching 5% of mass loss and causing a maximum cover crack value of 0.6 mm (Table 2). At nearly 9.8 days, a clear slope change in the curves of the number of hits and CSS can be seen in Figs. 2 and 3. This point of sudden AE activity can be related to the occurrence of corrosion initiation, which is followed by the onset of micro-cracking at the concrete-to-steel interface.

The analysis of AE parameters (number of hits and CSS) enabled the recognition of corrosion onset (increased AE activity) at times ranged between 9.8 and 10.7 days from all sensors in all beams. At these times, no visible signs of corrosion or cover cracks were noticed in any of the beams. To compare the AE detection of corrosion start in all beams, the half-cell potential (HCP) results were reviewed throughout the test periods, as demonstrated in Fig. 4. The HCP reading of more negative than -350 mV indicates more than 90% probability that reinforcing steel corrosion is occurring according to ASTM C876 [27]. Following this approach, the HCP tests detected corrosion initiation in all beams at 13-14 days from the beginning of test. These results manifested the capability of AE monitoring to detect corrosion initiation earlier than both the HCP method and visual observation of corrosion-induced cracks. This finding indicated that AE sensors have the ability to detect localized corrosion in RC beams within a range of damage location of 0.2 to 1.505 m.

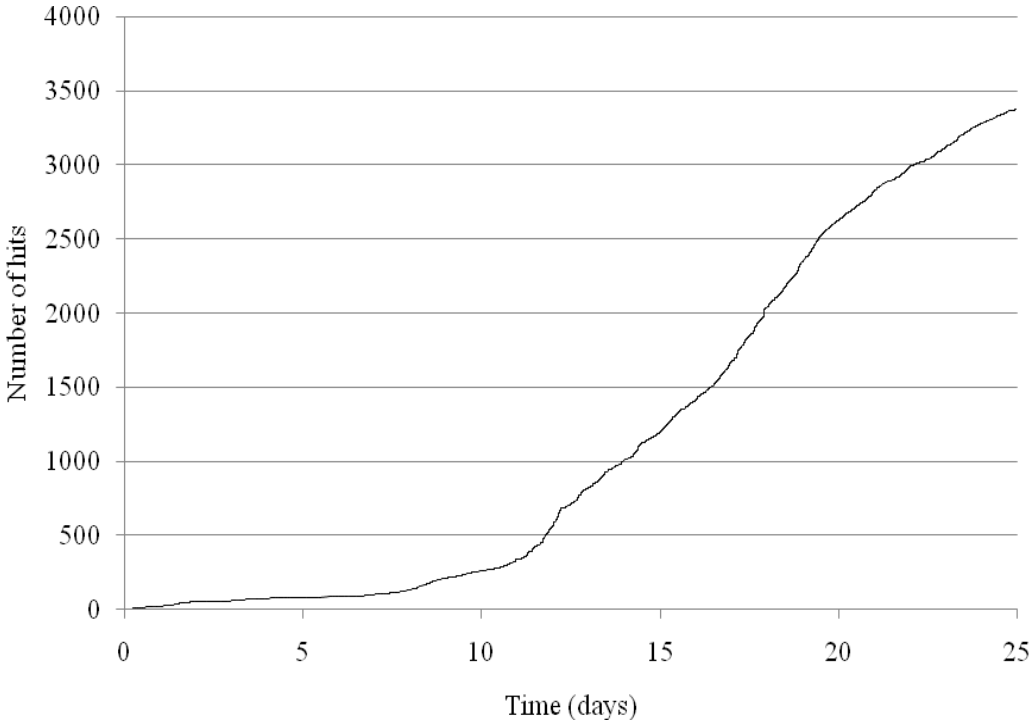

Fig. 2: Number of hits versus time of B1 Sensor 2.

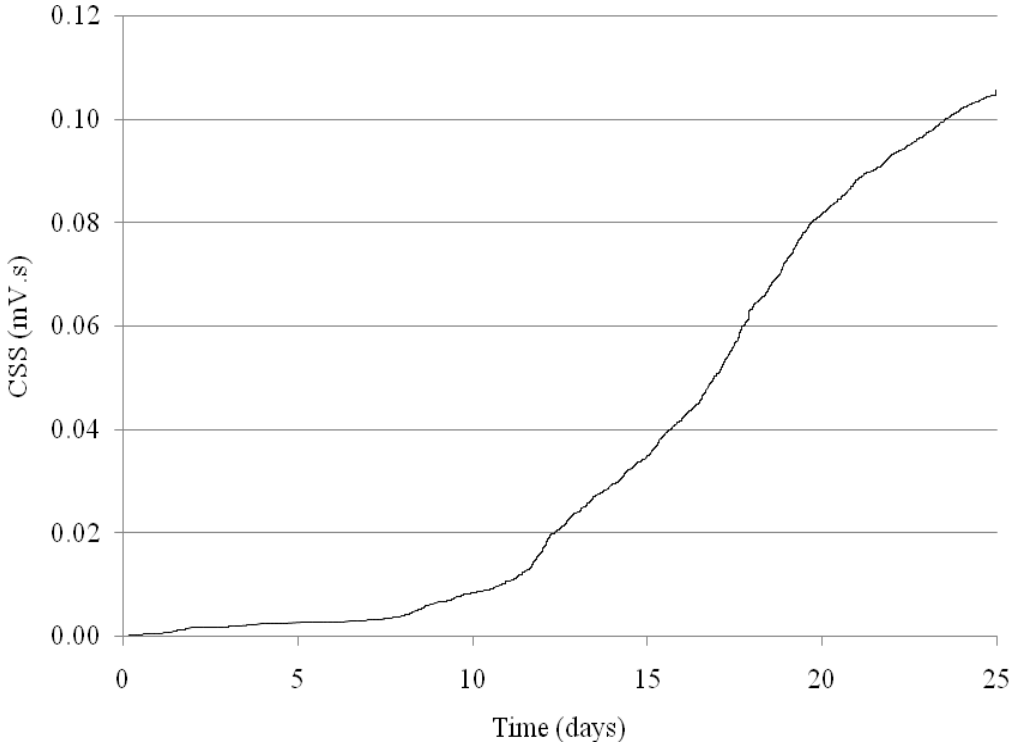

Fig. 3: CSS versus time of B1 Sensor 2.

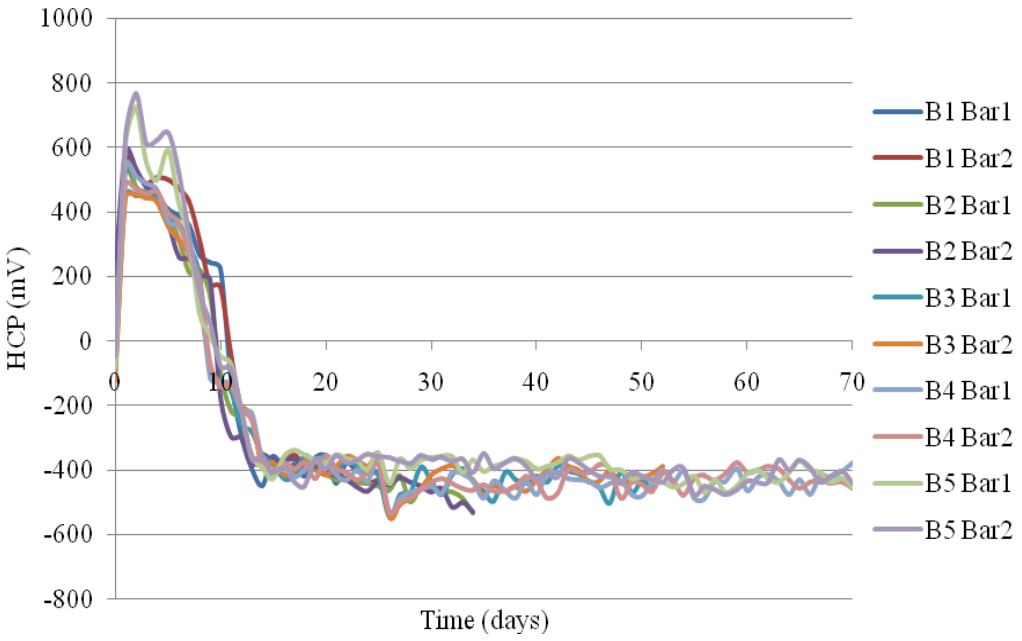

Fig. 4: HCP for all beams.

3.2. Early Corrosion-Induced Crack Detection by AE Analysis

After corrosion initiation, the analysis of the abovementioned AE parameters was continued to attain an early detection of cover cracking due to the expansive nature of corrosion products. The first visual crack was observed in all beams at 14-15 days from the beginning of the corrosion exposure in all beams (Table 2). A second clear slope change in the curves of the number of hits and CSS was also noticed, as demonstrated in Figs. 2 and 3. The high AE activity is mostly ascribed to the growth of macro-cracking leading to cover cracks, which were visually later observed at the side of all beams. It is worth noting that the growth of both micro- and macro-cracking is considered one of the important sources of acoustic emission. The identification of cover crack growth using the data from the three sensors in all beams was similarly performed and showed to occur at approximately 11.2-12.9 days. These results highlighted the effectiveness of the AE analysis in the prognosis of corrosion crack growth earlier than their visual observation in all beams, regardless of sensor location.

4. Conclusions

This article examined the feasibility of using AE monitoring in the early detection of reinforcement corrosion in large-scale RC beams. Five reinforced concrete beams were subjected to electrically accelerated corrosion tests and were continuously monitored via 3 attached AE sensors at varied distances from the source of damage. The analysis of the AE parameters acquired using these sensors and its comparison with the HCP tests and visual inspection of corrosion-induced cover cracks resulted in the following conclusions:

- The locations of slope change of the number of hits and CSS curves enabled the early detection of corrosion initiation and onset of corrosion-induced cover crack growth prior to both the HCP tests and visual observation of cracks in all beams, irrespective of sensor location.
- All sensors enabled the detection/characterization of corrosion initiation and onset of corrosion-induced cover crack in all beams with variable distances from the exposed bars ranged between 0.2 to 1.505 m.
- The distribution of AE sensors at larger distances than those covered in this study (> 1.505 m) requires further examination to identify the maximum allowable distance between sensors and to determine the minimum number of required sensors to capture the onset of corrosion in actual structures.
- The outcomes from this experimental study confirmed the feasibility of the AE analysis approach presented herein for detecting the corrosion inception in large-scale RC beams. Further investigations involving

testing RC structures exposed to natural corrosion process are recommended to enhance the reliability of the corrosion damage detection approach prior to application in actual RC structures.

5. References

[1] A. A. A. Hassan, K. M. A. Hossain and M. Lachemi (January 2009). Corrosion Resistance of Self-Consolidating Concrete in Full-scale Reinforced Beams. *Cement and Concrete Composites [Online]*. 31(1). pp. 29-38. Available: https://www.sciencedirect.com/science/article/pii/S0958946508001248

https://doi.org/10.1016/j.cemconcomp.2008.10.005

[2] H. S. Al-Alaily and A. A. A. Hassan (September 2016). Time-dependence of Chloride Diffusion for Concrete Containing Metakaolin. *Journal of Building Engineering [Online]*. 7. pp. 159-169. https://www.sciencedirect.com/science/article/pii/S2352710216300572

https://doi.org/10.1016/j.jobe.2016.06.003

[3] A. A. Abouhussien and A. A. A. Hassan (October 2014). Experimental and Empirical Time to Corrosion of Reinforced Concrete Structures under different Curing Conditions. *Advances in Civil Engineering [Online]*. 2014(Article ID 595743). pp. 1-9. Available: https://www.hindawi.com/journals/ace/2014/595743/abs/

[4] H. S. Al-Alaily, A. A. A. Hassan and A. A. Hussein (November 2017). Use of eXtended FEM and Statistical Analysis for modelling the corrosion-induced cracking in reinforced concrete containing metakaolin. *Canadian Journal of Civil Engineering [Online]*. 45(3). pp. 167-178. Available: http://www.nrcresearchpress.com/doi/abs/10.1139/cjce-2017-0298#.WqGyAWrwbIU

https://doi.org/10.1139/cjce-2017-0298

[5] H. S. Al-Alaily and A. A. A. Hassan (January 2018). A study on the Effect of Curing Temperature and Duration on Rebar Corrosion. *Magazine of Concrete Research [Online]*. 70(5). pp. 260-270. Available: https://www.icevirtuallibrary.com/doi/abs/10.1680/jmacr.17.00080

https://doi.org/10.1680/jmacr.17.00080

[6] A. A. A. Hassan, K. M. A. Hossain and M. Lachemi (March 2010). Structural Asessment of Corroded Self-consolidating Concrete Beams. *Engineering Structures [Online]*. 32(3). pp. 874-885. Available: https://www.sciencedirect.com/science/article/pii/S0141029609003976

https://doi.org/10.1016/j.engstruct.2009.12.013

[7] A. A. Abouhussien and A. A. A. Hassan (February 2015). Optimizing the Durability and Service Life of Self-consolidating Concrete Containing Metakaolin using Statistical Analysis. *Construction and Building Materials [Online]*. 76. pp. 297-306. Available: https://www.sciencedirect.com/science/article/pii/S0950061814013026

https://doi.org/10.1016/j.conbuildmat.2014.12.010

[8] H. S. Al-alaily, A. A. Abouhussien and A. A. A. Hassan (June 2017). Influence of Metakaolin and Curing Conditions on Service Life of Reinforced Concrete. *Journal of Materials in Civil Engineering [Online]*. 29(10). pp. 04017161. Available: https://ascelibrary.org/doi/full/10.1061/(ASCE)MT.1943-5533.0002010

https://doi.org/10.1061/(ASCE)MT.1943-5533.0002010

[9] A. A. Abouhussien and A. A. A. Hassan, "Experimental Study on Corrosion Monitoring and Assessment of Concrete Structures Using Acoustic Emission," in *Proc. International Conference on Advances in Structural and Geotechnical Engineering, ICASGE'15, Hurghada, Egypt*, 2015, pp. 1-8.

[10] H. S. Al-Alaily, A. A. A. Hassan and A. A. Abouhussien "Experimental Study on Service Life of Concrete Under Severe Corrosion Environment," in *Proc. 4th Specialty Conference on Coastal, Estuary and Offshore Engineering, Canadian Society for Civil Engineering, CSCE Annual Conference 2013, Montréal, Québec, Canada*, 2013, pp. 1-11.

[11] W. Vélez, F. Matta and P. Ziehl (November 2014). Acoustic Emission Monitoring of Early Corrosion in Prestressed Concrete Piles. *Structural Control and Health Monitoring [Online]*. 22(5). pp. 873-887. Available: http://onlinelibrary.wiley.com/doi/10.1002/stc.1723/abstract

https://doi.org/10.1002/stc.1723

[12] S. Patil, B. Karkare and S. Goyal (October 2014). Acoustic emission vis-à-vis electrochemical techniques for corrosion monitoring of reinforced concrete element. *Construction and Building Materials [Online]*. 68. pp. 326-332. Available: https://www.sciencedirect.com/science/article/pii/S0950061814006874

https://doi.org/10.1016/j.conbuildmat.2014.06.068

[13] A. Zaki, H. K. Chai, D. G. Aggelis and N. Alver (August 2015). Non-destructive evaluation for corrosion monitoring in concrete: A review and capability of acoustic emission technique. *Sensors [Online]*. 15(8). pp. 19069–19101. Available: https://www.ncbi.nlm.nih.gov/pmc/articles/PMC4570360/

https://doi.org/10.3390/s150819069

[14] M. Di Benedetti, G. Loreto, F. Matta and A. Nanni (October 2013). Acoustic emission historic index and frequency spectrum of reinforced concrete under accelerated corrosion. *Journal of Materials in Civil Engineering [Online]*. 26(9). pp. 04014059. Available: https://ascelibrary.org/doi/abs/10.1061/(ASCE)MT.1943-5533.0000954

https://doi.org/10.1061/(ASCE)MT.1943-5533.0000954

[15] A. A. Abouhussien and A. A. A. Hassan (November 2015). Evaluation of damage progression in concrete structures due to reinforcing steel corrosion using acoustic emission monitoring. *Journal of Civil Structural Health Monitoring [Online]*. 5(5). pp. 751-765. Available: https://link.springer.com/article/10.1007/s13349-015-0144-5

https://doi.org/10.1007/s13349-015-0144-5

[16] A. A. Abouhussien and A. A. A. Hassan, "Cover crack growth monitoring in RC structures subjected to corrosion with acoustic emission sensors," in *Proc. 5th International Structural Specialty Conference, Canadian Society for Civil Engineering, CSCE Annual Conference 2016, London, Ontario, Canada*, 2016, pp. 1-10.

[17] A. A. Abouhussien and A. A. A. Hassan (September 2016). The use of acoustic emission intensity analysis for the assessment of cover crack growth in corroded concrete structures. *Journal of Nondestructive Evaluation [Online]*. 35 (3). 52. Available: https://link.springer.com/article/10.1007/s10921-016-0369-1

https://doi.org/10.1007/s10921-016-0369-1

[18] A. A. Abouhussien and A. A. A. Hassan, "Assessment of concrete-to-steel bond behaviour of reinforced concrete structures using acoustic emission intensity analysis," in *Proc. 11th International Conference on Civil and Architecture Engineering, ICCAE-11, Cairo, Egyp*t, 2016, pp. 1-22.

[19] A. A. Abouhussien and A. A. A. Hassan, "Condition assessment of corroded reinforcement bond to concrete by acoustic emission monitoring," in *Proc. 5th International Structural Specialty Conference, Canadian Society for Civil Engineering, CSCE Annual Conference 2016, London, Ontario, Canada*, 2016, pp. 1-10.

[20] A. A. Abouhussien and A. A. A. Hassan (November 2016). Acoustic emission monitoring for bond integrity evaluation of reinforced concrete under pull-out tests. *Advances in Structural Engineering [Online]*. 20 (9). 1390-1405. Available: http://journals.sagepub.com/doi/abs/10.1177/1369433216678864

https://doi.org/10.1177/1369433216678864

[21] A. A. Abouhussien and A. A. A. Hassan (May 2016). Acoustic emission-based analysis of bond behavior of corroded reinforcement in existing concrete structures. *Structural Control and Health Monitoring [Online]*. 24(3). e1893. Available: http://onlinelibrary.wiley.com/doi/10.1002/stc.1893/full

https://doi.org/10.1002/stc.1893

[22] A. A. Abouhussien and A. A. A. Hassan (June 2016). Detection of bond failure in the anchorage zone of reinforced concrete beams via acoustic emission monitoring. *Smart Materials and Structures [Online]*. 25(7). pp. 075034. Available: http://iopscience.iop.org/article/10.1088/0964-1726/25/7/075034

https://doi.org/10.1088/0964-1726/25/7/075034

[23] A. A. Abouhussien and A. A. A. Hassan (November 2016). Application of acoustic emission monitoring for assessment of bond performance of corroded reinforced concrete beams. *Structural Health Monitoring [Online]*. 16 (6). 732-744. Available: http://journals.sagepub.com/doi/abs/10.1177/1475921716681460

https://doi.org/10.1177/1475921716681460

[24] ASTM (2017) C 150: Standard specification for portland cement. ASTM International, West Conshohocken, PA, USA.

[25] ASTM (2012) C 39: Standard test method for compressive strength of cylindrical concrete specimens. ASTM International, West Conshohocken, PA, USA.

[26] ASTM (2011) C 496: Standard test method for splitting tensile strength of cylindrical concrete specimens. ASTM International, West Conshohocken, PA, USA.

[27] ASTM (1991) C 876: Standard test method for half-cell potentials of uncoated reinforcing steel in concrete. ASTM International, West Conshohocken, PA, USA.

[28] ASTM (2011) G 1: Standard practice for preparing, cleaning, and evaluating corrosion test specimens. ASTM International, West Conshohocken, PA, USA.